EDGE ARTICLE

CrossMark
← click for updates

The application of chiroptical spectroscopy (circular dichroism) in quantifying binding events in lanthanide directed synthesis of chiral luminescent self-assembly structures†

Oxana Kotova,*[a] Salvador Blasco,[a] Brendan Twamley,[a] John O'Brien,[a] Robert D. Peacock,[b] Jonathan A. Kitchen,[ac] Miguel Martínez-Calvo[a] and Thorfinnur Gunnlaugsson*[a]

The binding of asymmetrical and optically pure tridentate ligands (L = **1(S)** and **1(R)**) containing one carboxylic group and 2-naphthyl as an antenna to lanthanide ions (M = La(III) and Eu(III)) was studied in CH_3CN, showing the successive formation of M:L, M:L$_2$ and M:L$_3$ stoichiometric species in solution. The europium complexes EuL$_3$ were also synthesised, structurally characterised and their photophysical properties probed in CH_3OH and CH_3CN. The changes in the chiroptical properties of both **1(S)** and **1(R)** were used (by circular dichroism (CD) spectroscopy) to monitor the formation of these chiral self-assemblies in solution. While circularly polarised luminescence (CPL) showed the formation of Eu(1(S))$_3$ and Eu(1(R))$_3$ as enantiomers, with high luminescence dissymmetry factors (g_{lum}), fitting the CD changes allowed for binding constants to be determined that were comparable to those seen in the analyses of absorbance and luminescence changes.

Introduction

Due to the many unique spectroscopic properties that the lanthanides (Ln) possess, such as long-lived excited states and long emission wavelength, the synthesis of novel luminescent lanthanide based self-assemblies has led to the development of various novel optical and functional materials in recent times.[1] Examples of such developments are the formation of supramolecular self-assembly structures, such as helicates and interlocked lanthanide-based catenanes,[1e,f] luminescent sensors for ions and molecules, probes for cellular imaging and for observing biological process and as supramolecular polymers.[2] Chiral lanthanide complexes have been developed increasingly for such applications.[3,4] We have developed numerous examples of chiral ligands that have been employed in lanthanide directed synthesis of self-assembled architectures. These have been based on the dipicolinic acid motive (**H₂dpa**)[5] which has been shown to be an efficient sensitiser for Eu(III) and Tb(III) luminescence.[6] Moreover, as we and others have demonstrated, the carboxylic groups can be synthetically

modified easily with various chiral or achiral antennae to give cationic lanthanide complexes.[7–12] In related work, both Bünzli and De Cola have recently demonstrated that mono-anionic asymmetrical ligands containing three donor atoms can form stable charge neutral complexes with various lanthanides.[13] Herein we present ligands **1(S)** and **1(R)** (Scheme 1) based on the **H₂dpa** core, each ligand possessing a single chiral (*S*)- and

[a]*School of Chemistry, Trinity Biomedical Sciences Institute, Trinity College Dublin, Dublin 2, Ireland. E-mail: kotovao@tcd.ie; gunnlaut@tcd.ie*
[b]*School of Chemistry, University of Glasgow, Glasgow, G12 8QQ, Scotland, UK*
[c]*Chemistry, University of Southampton, Southampton, SO17 1BJ, UK*
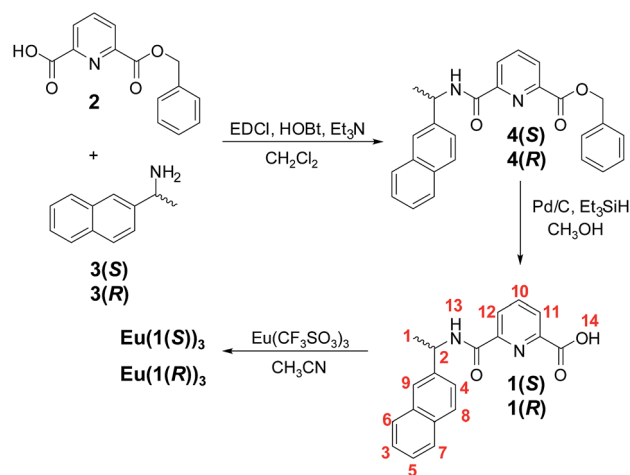
Scheme 1 Synthesis of the ligands **1(S)** and **1(R)**, and their corresponding complexes Eu(1(S))$_3$ and Eu(1(R))$_3$ synthesized under microwave irradiation.

(*R*)-1-(2-naphthyl)-ethylamine antenna, respectively. Both Eu(III) complexes were formed from these ligands using a synthesis under microwave irradiation and the photophysical properties of the resulting complexes **Eu(1(*S*))₃** and **Eu(1(*R*))₃** studied in CH₃CN and CH₃OH solutions. Self-assembly of these ligands with Ln(III) was studied in CH₃CN solution by monitoring the changes in both ground and excited states (Ln = Eu(III)) as well as by NMR spectroscopy (Ln = La(III)). Due to the chiral nature of the ligands and concomitant formation of chiral Ln-complexes in solution upon titration with Ln(III), we studied their chiroptical properties using both CD and CPL spectroscopies. The crystallographic analysis of **Eu(1(*R*))₃** confirmed that the chirality of the ligand was transferred to the Eu(III) centre. Adequately, the changes in CD spectra of either **1(*S*)** and **1(*R*)** were drastically affected upon binding to Eu(III); being equal magnitude but of opposite signs. This allowed us to identify both the different **Ln$_x$:L$_y$** stoichiometries in solution and to quantify their binding affinities using non-linear regression analysis, in a similar manner to that used to quantify the same in both the absorption and the luminescence titrations. While CD spectroscopy is commonly used to monitor the interaction, formation or folding of larger self-assembly structures in solution,[14] to the best of our knowledge, carrying out CD titrations to assess the different equilibrium processes for the formation of chiral self-assembly metal ion complexes and determination of the affinity constants for such processes is relatively unexplored in supramolecular chemistry. Here we demonstrate that indeed such analysis gives greater understanding of the different stoichiometric speciation in solution and that the binding constants determined for these matched comfortably well with that determined by traditional spectroscopic methods.

Results and discussion

Synthesis of the ligands and Eu(III) complexes

The tridentate ligands **1(*S*)** and **1(*R*)** were synthesised in three steps starting from commercially available **H₂dpa**. First the dipicolinic acid was monoprotected with benzylbromide to give **2** in 38% yields (see ESI†).[15] This was further coupled, Scheme 1, with either (*S*)- or (*R*)-1-(2-naphthyl)-ethylamine (**3(*S*)** or **3(*R*)**, respectively) using standard peptide-coupling methodology[9b] in presence of 1-(3-dimethylaminopropyl)-3-ethylcarbodiimide hydrochloride (EDCI·HCl) and 1-hydroxybenzotriazole hydrate (HOBt) to give the intermediates **4(*S*)** and **4(*R*)** in *ca.* 80% yield for both. The deprotection of the benzyl esters **4(*S*)** and **4(*R*)** was first attempted by catalytic hydrogenation using 10% Pd/C catalyst. However, this resulted in the product containing impurities that were difficult to isolate from the desired products. For this reason we turned to the use of Pd–C-induced catalytic transfer hydrogenation using triethylsilane[16] which gave desired products **1(*S*)** and **1(*R*)** in *ca.* 78% yield for both. The ¹H NMR spectrum of **1(*S*)** is shown in Fig. 1, demonstrating the successful deprotection of the benzyl ester (the same result observed for **1(*R*)**; see ESI†). High resolution electrospray mass-spectrometry (see ESI†) also confirmed the successful formation of both ligands with of *m/z* = 319.1075 for **1(*S*)** and 319.1080 for
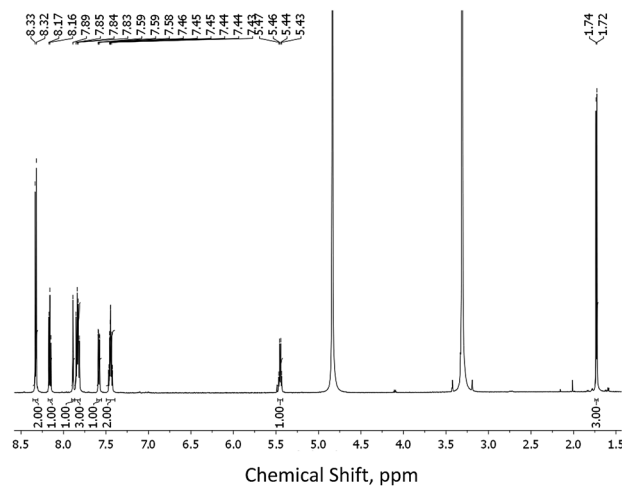

Fig. 1 ¹H NMR of **1(*S*)** (600 MHz, CD₃OD).

1(*R*) corresponding to [M − H⁺]⁻, while the IR spectra revealed the presence of characteristic C–H, N–H and C=O vibrations. The results of the elemental analysis also confirmed the formation of the pure compounds. We were also able to grow single crystals suitable for X-ray crystal structure analysis of both **4(*S*)** and **4(*R*)** by recrystallization of powder samples from methanol. Similarly, single crystals of **1(*S*)** and **1(*R*)** were grown from a mixture of CH₃OH and CH₃CN and the low temperature (100(2) K) X-ray structures collected. These will be discussed in the next section.

Having obtained both **1(*S*)** and **1(*R*)** we next synthesised the Eu(III) complexes **Eu(1(*S*))₃** and **Eu(1(*R*))₃** from these, where each of the ligand is expected to coordinate to the lanthanide *via* the central pyridine nitrogen, the carboxylic acid and the carboxylic amide, in a tri-dentate manner. Three of these ligands therefore fulfil the high coordination requirements of the lanthanide. This was achieved by reacting Eu(CF₃SO₃)₃ with **1(*S*)** and **1(*R*)** in a 1 : 3 metal to ligand stoichiometry in CH₃CN solution under microwave irradiation at 95 °C for 30 minutes. The resulting complexes were isolated as white powders by slow diffusion of diethyl ether into the CH₃CN solutions, yielding the desired complexes in *ca.* 35% yields. High resolution matrix-assisted laser desorption/ionization (MALDI) mass-spectrometry confirmed the formation of both tris-chelates with the presence of *m/z* = 1147.2034 which was assigned to [Eu(**1(*S*)**–H⁺)₃ + K⁺]⁺ and 1147.2039, assigned to [Eu(**1(*R*)**–H⁺)₃ + K⁺]⁺ (see ESI†). The ¹H NMR (CD₃CN, 600 MHz) spectra for both Eu(III) complexes were different to that of the free ligands showing significant broadening and shift of the proton resonances (see ESI†), due to the paramagnetic nature of the lanthanide ion. Similarly, in the IR spectra, the C=O vibronic transitions were significantly shifted by 126 cm⁻¹ upon complexation to Eu(III), further confirming the complex formation. Elemental analysis also confirmed the formation of the desired products. However, the latter, along with the MALDI results, suggests that partial deprotonation of the ligands upon complexation occurs, which is not surprising since the carboxylic acid is directly bound to the lanthanide, making it more acidic. Both complexes were

also shown to be luminescent, as upon placing a solution of both under a UV light irradiation red emission characteristic of Eu(III) was observed, confirming that the ligands functions as sensitising antennae for the $^5D_0$ excited state of Eu(III). Clear colourless crystals of **Eu(1(R))₃** were obtained as described previously by Bünzli et al.[13a–c]

The coordination geometry of the Eu(III) centres was first evaluated in solution by measuring the decay of the lanthanide excited state in both H_2O and D_2O, upon excitation at the naphthalene antennae ($\lambda_{ex} = 281$ nm) allowing for the determination of the Eu(III) hydration state (q, the number of metal-bound water molecules).[17] The Eu(III) $^5D_0$ excited state life-times of **Eu(1(S))₃** were best-fitted to monoexponential decay with $\tau_{H_2O} = 1.54 \pm 0.01$ ms and $\tau_{D_2O} = 2.57 \pm 0.01$ ms giving a q value of zero. This is to be expected as the lanthanides have coordination requirements of 8–10, these being fulfilled by the 9 coordination environment of the 1 : 3 **Eu:L** stoichiometry in **Eu(1(S))₃**.[11] Similarly, the Eu(III) excited state life-times of **Eu(1(R))₃** were best fitted to monoexponential decay with $\tau_{H_2O} = 1.55 \pm 0.01$ ms and $\tau_{D_2O} = 2.50 \pm 0.04$ ms, again confirming that the ions were complexed with saturation of coordination environment.

Crystal and molecular structures of 4(S), 4(R), 1(S), 1(R) and Eu(1(R))₃

As stated above, crystalline materials of both **1(R)** and **1(S)** were obtained that allowed for the X-ray analysis of these enantiomers. The resulting structures are shown in Fig. 2A and B, respectively. Each enantiomer crystallizes in the chiral space group $P2_1$ and displays two different independent molecules in the asymmetric unit. The chiral centres are C13 and C37, and although the chirality was known throughout the syntheses, it was confirmed by the refined Flack parameter for each enantiomer. The two independent molecules differ by rotation of the naphthyl group around the C13–C15 (C37–39) bond (torsion angle C14–C13–C15–C16, C38–C37–C39–C40; **1(R)** = −19.5(2), 9.3(2): **1(S)** = 19.84(17), −9.50(17)°). The structures of **4(S)** and **4(R)**, again in the chiral space group $P2_1$, were obtained from enantiopure crystals grown from methanol solutions, see Fig. 2C and D, respectively. Here the asymmetric unit consists of a single molecule. The additional substitution on the carboxyl group leads to a planar pyridine–C(O)O–CH₂–Ph unit (**4(S)**, **4(R)** = 0.04 Å deviation from plane). The chiral centre is C11 and was confirmed by the Flack parameter. The naphthyl groups are rotated about the C10–C11 bond with C9–C10–C11–C12 torsion angles of **4(R)**: −62.7(2) and **4(S)**: 62.8(2)°. The chiral subunit (R–C(O)NHCMe–naphthyl) seen in **1(R)**, **1(S)**, **4(S)** and **4(R)** has been structurally characterized previously and displays a wide range of naphthyl group: chiral centre arrangements.[18]

In both **1(S)** and **1(R)**, strong hydrogen bonding was observed between the carboxylic acid group and the carbonyl group of neighbouring ligand. This orientation results in other weak inter- and intra- molecular hydrogen bonding between the back-to-back molecules (see Table 1) and creates a weakly connected supramolecular ribbon motif parallel to the c-axis. In **4(S)** and **4(R)** the hydrogen bonding motif is disrupted by the substitution on the carboxyl group. In this case only weak C–H⋯O interactions prevail.

The complex **Eu(1(R))₃** (Fig. 3, ESI†) crystallized in an orthorhombic crystal system with chiral space group $C222_1$ (Table 1). The asymmetric unit contains two different **Eu(1(R))₃** molecules and some water molecules. The ligands are arranged around Eu(III) ion in a manner predicted by us previously for the complexes formed from the use of ligands with 1-naphthyl group as an antenna (assigned here as **Eu(5(S))₃** and **Eu(5(R))₃**, see ESI† for structure)[11] and observed by others[13] with three naphthyl antennae located on the same side (Fig. 3A). As observed previously ($q = 0$) and confirmed here, the coordination environment of Eu(III) centre in either of the molecules is
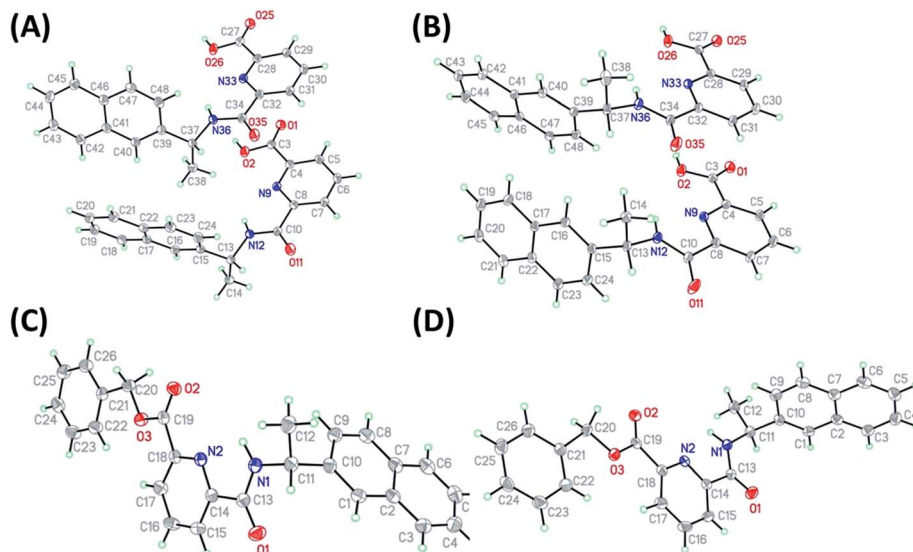

Fig. 2 Molecular structures of (A) **1(R)** and (B) **1(S)** showing both independent molecules in the asymmetric unit, (C) **4(R)** and (D) **4(S)** (thermal displacement 50%).

Table 1 Summary of crystallographic details for compounds **1(S)**, **1(R)**, **4(S)**, **4(R)** and **Eu(1(R))₃**

Compound reference	**1(R)**	**1(S)**	**4(R)**	**4(S)**	**Eu(1(R))₃**
Chemical formula	$C_{19}H_{16}N_2O_3$	$C_{19}H_{16}N_2O_3$	$C_{26}H_{22}N_2O_3$	$C_{26}H_{22}N_2O_3$	$C_{57}H_{49.5}EuN_6O_{11.5}$
Formula mass	320.34	320.34	410.45	410.45	1159.49
Crystal system	Monoclinic	Monoclinic	Monoclinic	Monoclinic	Orthorhombic
$a/\text{Å}$	6.8436(4)	6.8507(4)	5.4249(2)	5.4288(2)	26.0015(12)
$b/\text{Å}$	26.8023(14)	26.7770(17)	16.5948(6)	16.6067(6)	26.4029(11)
$c/\text{Å}$	8.3932(5)	8.4103(5)	11.4170(4)	11.4114(4)	30.8305(11)
$\beta/°$	90.9000(13)	90.840(2)	98.277(2)	98.2867(18)	90
Unit cell volume/Å^3	1539.33(15)	1542.63(16)	1017.11(6)	1018.05(6)	21165.6(15)
Temperature/K	100(2)	100(2)	100(2)	100(2)	100(2)
Space group	$P2_1$	$P2_1$	$P2_1$	$P2_1$	$C222_1$
No. of formula units per unit cell, Z	4	4	2	2	16
Radiation type	MoKα	MoKα	CuKα	CuKα	CuKα
Absorption coefficient, μ/mm^{-1}	0.095	0.095	0.710	0.709	9.05
No. of reflections measured	24 241	47 256	5614	5359	36 491
No. of independent reflections	6995	10 624	2414	2462	9417
R_{int}	0.0171	0.0145	0.0273	0.0303	0.0740
Final R_1 values ($I > 2\sigma(I)$)	0.0254	0.0321	0.0306	0.0309	0.083
Final w$R(F^2)$ values ($I > 2\sigma(I)$)	0.0646	0.0861	0.0806	0.0762	0.262
Final R_1 values (all data)	0.0268	0.0339	0.0307	0.0310	0.1512
Final w$R(F^2)$ values (all data)	0.0654	0.0873	0.0808	0.0763	0.2618
Goodness of fit on F^2	1.039	1.035	1.068	1.055	1.006
Flack parameter	0.0(2)	0.31(11)	−0.11(7)	−0.15(9)	−0.001(8)
CCDC number	999267	999268	999269	999270	1026036

fully saturated with three molecules of deprotonated **1(R)** contributing with three coordination bonds each being the pyridine nitrogen flanked by the carboxylate oxygen on one side and the amido oxygen on the other side. Both europium atoms are positioned in a nine-coordinated tri-capped trigonal prismatic N_3O_6 coordination environment formed by the three pyridine nitrogen atoms located in the equatorial plane arranging in quite regular triangle, and six oxygen atoms where three are placed above while the other three lay below the equatorial plane forming a triangular prism among them. Thus, the complex remains C_3 symmetry. The average bond distances are 2.37 Å for Eu–O(carboxylate) bonds, 2.44 Å for Eu–O(amido) and 2.57 Å for Eu–N(pyridine). The chirality of the ligand, known from the synthesis, is also confirmed in this structure by the Flack parameter.

The naphthalene moieties interact with each other and with the pyridine groups *via* π-stacking and they form hydrophobic pockets in the structure. Multiple intramolecular and inter-molecular π-stacking interactions can be observed in the fragment containing the Eu1 atom, the naphthalene C48–C57 interacts face to face with pyridine N3–C21–C25 and edge to face with naphthalene C29–C38 but this pyridine also interacts face to face with the naphthalene C10–C19 (Fig. 3B, ESI†). Similar interactions can be seen in the other fragment (the one that contains the Eu2 atom) with the pyridine N9–C78–C82 in between the naphthalene group C67–C76 and C116–C125. Naphthalene groups have some conformational freedom and they can, at some extent rock and rotate and as a result high disorder is found in these moieties. In the case of the naphthalene group attached to C(103) it has been found in two different orientations with occupancy factor 1/2.
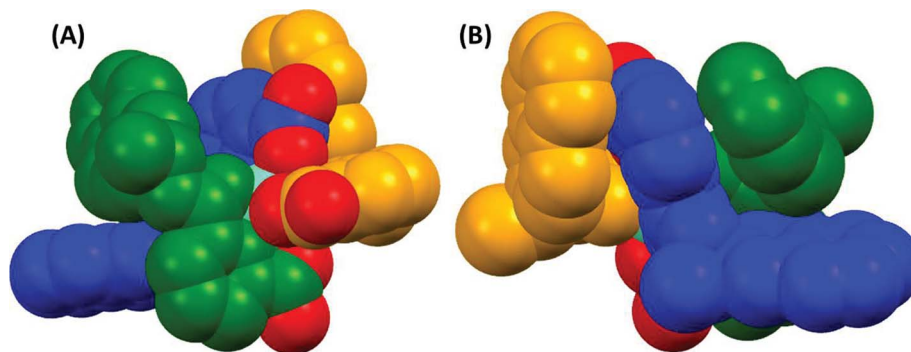

Fig. 3 Space filling representation of **Eu(1(R))₃** complex showing (A) the position of carboxyl oxygen atoms (in red) relatively to naphthyl antennae and (B) stacking interaction between pyridine and naphthyl groups.

Photophysical properties of Eu(III) complexes in CH₃CN and CH₃OH solutions

Having structurally characterised the ligands and their corresponding complexes, we next investigated their photophysical properties. The electronic absorption spectra of the ligands in CH₃CN (see ESI†) were dominated by ligand-centred n → π* and π → π* transitions centred at 222 nm (**1(S)**: $\varepsilon = 87\,397 \pm 230$ cm^{-1} M^{-1}; **1(R)**: $\varepsilon = 87\,158 \pm 320$ cm^{-1} M^{-1}) and 270 nm (**1(S)**: $\varepsilon = 10\,964 \pm 38$ cm^{-1} M^{-1}; **1(R)**: $\varepsilon = 11\,630 \pm 146$ cm^{-1} M^{-1}). The excitation into the 270 nm transition did not result in any significant ligand centred emission. However, upon complexation to the metal ion significant Eu(III)-centred emission was observed due to the energy transfer processes occurring from the 2-naphthyl antennae to the $^5D_0$ excited state which was followed by deactivation to the ^7F_J bands of the lanthanide. The photophysical properties of **Eu(1(S))₃** and **Eu(1(R))₃** were also studied in CH₃OH and compared to that observed for **Eu(5(S))₃** and **Eu(5(R))₃** (ESI†).[11] The results are shown in Table 2 and it was demonstrated that the structure of Eu(III)-centred emission bands is similar for both, confirming that these systems have similar coordination environments of the metal centre. The photoluminescence quantum yields (Φ_{tot}, %) were also measured by a relative method using Cs₃[Eu(**dpa**)₃]·9H₂O as a standard.[19] In general, the quantum yields of the 1-naphthyl derivatives were *ca.* 4 times higher in CH₃CN and 2 times higher in CH₃OH than seen for the 2-naphthyl analogues. Based on our previous work, where we investigated the symmetrical Eu(III) "Trinity Sliotar" complexes,[8] we believe that this difference is due to sensitisation efficiency of Eu(III) luminescence being more favourable for **Eu(5(S))₃** and **Eu(5(R))₃** than **Eu(1(S))₃** and **Eu(1(R))₃**. This is evident from calculating the antenna-to-ion energy transfer efficiencies (η_{sens}) for these complexes, which is determined on the basis of the emission spectrum, the observed luminescence life-time (τ_{obs}) and the experimental overall luminescence quantum yield (Φ_{tot}) upon ligand excitation, Table 2.

The quantum yield of the Eu(III) complexes in CH₃OH solution was found to be significantly lower than that seen in CH₃CN, which we contribute to a dissociation of these complexes in more competitive protic media, where one of the ligands is removed from the **EuL₃** complex to give **EuL₂** + **L**. The latter now being affected by quenching of the lanthanide excited state by energy matching solvent O–H oscillators. The Eu(III)-centred emission decays for both groups of complexes were found to be bi-exponential with the main species being **EuL₃** (~80%) for the complexes with **1(S)** and **1(R)** while in case of 1-naphthyl derivatives **EuL₂** species (~80%) were prevalent (Table 2). Interestingly, the values of Φ_{tot} and τ_{obs} between symmetrical "Trinity Sliotar"[8] and the asymmetrical Eu(III) complexes (**Eu(1(S))₃** and **Eu(1(R))₃**) developed herein and that of **Eu(5(S))₃** and **Eu(5(R))₃**)[11] in CH₃CN are found to be very similar. However, if one compares the ratio between $^5D_0 \rightarrow {}^7F_J$ transitions in the Eu(III)-centred emission spectra of these two sets of complexes it is possible to identify common differences which suggest discrepancy in the Eu(III) ion site symmetry within these two systems. In turn, τ_R of the symmetrical complexes was found to be higher as the shielding of the metal centre is better in this case compared to that seen for the asymmetrical structures. Hence, the values of Φ_{Ln}^{Ln} were found to be higher for asymmetrical molecules **Eu(1(S))₃**, **Eu(1(R))₃** and **Eu(5(S))₃**, **Eu(5(R))₃**, suggesting the larger influence of non-radiative processes in the symmetrical complexes. Finally, η_{sens} was higher for the symmetrical complexes as the asymmetrical lose one antenna per ligand. Having probed the photophysical properties of **Eu(1(S))₃** and **Eu(1(R))₃** we next turned our attention to analysing the role of the Eu(III) ion in the metal directed synthesis of these complexes under kinetic control at room temperature.

Monitoring self-assembly processes between 1(S) and 1(R) with Eu(III) in CH₃CN by absorption and luminescence spectroscopy

The self-assembly studies between **1(S)** or **1(R)** and Eu(III) were first performed in CH₃CN solution. However, the analysis of the data using non-linear regression analysis program SPECFIT® did not result in data convergence. As the self-assembly

Table 2 Antenna-to-ion energy transfer efficiencies (η_{sens}) of Eu(III) complexes calculated on the basis of the observed emission spectrum, the observed luminescence life-time (τ_{obs}) and the experimental overall luminescence quantum yield (Φ_{tot}) upon ligand excitation ($\lambda_{ex} = 279$ nm). τ_R is the radiative life-time calculated using eqn (3) (see EP). Φ_{Ln}^{Ln} is found using eqn (4) (see EP) measured in CH₃CN and CH₃OH

Complex	τ_{obs}, ms	Φ_{tot}, %	τ_R, ms	Φ_{Ln}^{Ln}, %	η_{sens}, %	Solvent/c, M
Eu(1(R))₃	1.86 ± 0.02	2.1 ± 0.1	6.43 ± 0.04	28.94 ± 0.01	7.26 ± 0.02	CH₃CN 2.72 × 10⁻⁵ M
Eu(1(S))₃	1.86 ± 0.02	1.6 ± 0.5	6.39 ± 0.04	29.13 ± 0.01	5.49 ± 0.02	
Eu(5(R))₃	1.94 ± 0.01	8.2 ± 0.3	7.13 ± 0.02	27.22 ± 0.01	30.20 ± 0.03	
Eu(5(S))₃	1.94 ± 0.01	8.4 ± 0.3	7.18 ± 0.04	27.02 ± 0.03	30.90 ± 0.01	
Eu(1(R))₃	0.58 ± 0.01 (18.8%)	0.6 ± 0.1	—	—	—	CH₃OH 5.79 × 10⁻⁵ M
	1.95 ± 0.01 (81.2%)					
Eu(1(S))₃	0.58 ± 0.01 (18.8%)	0.5 ± 0.1	—	—	—	
	1.95 ± 0.01 (81.2%)					
Eu(5(R))₃	0.58 ± 0.01 (79.0%)	2.2 ± 0.2	—	—	—	
	1.76 ± 0.03 (21.0%)					
Eu(5(S))₃	0.57 ± 0.01 (81.0%)	2.3 ± 0.1	—	—	—	
	1.58 ± 0.01 (19.0%)					
	0.57 ± 0.01 (81.0%)					

processes are highly dependent on the solvent and ions in solution, it was decided to introduce ionic strength into the system, as it has been shown by Piguet *et al.*[20] that the introduction of tetrabutylammonia perchlorate favours the formation of highly charged complexes in lanthanide-directed self-assemblies formations in aprotic solvent systems. Hence, to overcome the data convergence problem we choose to use 0.05 M tetraethylammonium chloride $((C_2H_5)_4NCl)$ as ionic strength in our studies.

The changes observed in the absorption, fluorescence and Eu(III)-centred emission spectra upon titrating **1(S)** and **1(R)** with Eu(III) were identical for both enantiomers and as such the discussion herein will focus only on one of these ligands. The changes seen upon titrating **1(S)** are shown in Fig. 4 (see ESI† for **1(R)**). As described previously, the absorption spectrum of **1(S)** possesses two main maxima at 222 and 270 nm (Fig. 4A). The addition of Eu(III) resulted in hyperchromicity in these absorption bands, where the main changes were observed in the bands centred at ~270 nm, as demonstrated in Fig. 5A, where the changes at three different transitions are plotted against added Eu(III) equivalents. Here, the absorbance increase was initially observed until addition of 0.30 equivalents of Eu(III), signifying the formation of the desired 1 : 3 stoichiometry, after which much slower increase occurred until the addition of 1.00 equivalents before beginning to plateau. The experimental changes were analysed using non-linear regression analysis program SPECFIT® (ref. 21) where factor analysis confirms the presence of four absorbing species. These were assigned to the ligand (**L**) and the Eu(III) species **M:L**, **M:L₂** and **M:L₃**. The data was satisfactorily fitted to the following equilibria and the associated binding constants, expressed as $\log \beta_{x:y}$, are summarised in Table 3:

$$Eu + L \leftrightarrow EuL \quad (\log \beta_{1:1})$$

$$Eu + 2L \leftrightarrow EuL_2 \quad (\log \beta_{1:2})$$

$$Eu + 3L \leftrightarrow EuL_3 \quad (\log \beta_{1:3})$$

These binding constants are comparable to that seen for structurally similar self-assemblies,[11,22] though not as high as

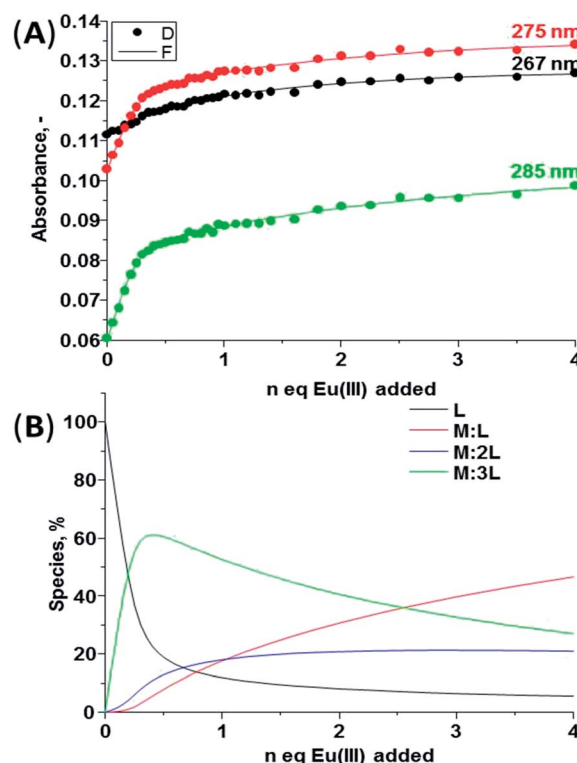
Fig. 5 (A) Experimental binding isotherms and their corresponding fit obtained using non-linear regression analysis program SPECFIT®, (B) speciation-distribution diagram obtained from the fit of the changes in the absorption spectrum of **1(S)** upon addition of $Eu(CF_3SO_3)_3$ in CH_3CN (25 °C, 0.05 M $(C_2H_5)_4NCl$).

that seen for analogues "Trinity Sliotar" complexes.[8–12] The speciation distribution diagram for the titration is shown in Fig. 5B, which demonstrates the initial formation of 1 : 3 (**M:L**) species in *ca.* 60% yield upon addition of 0.30 equivalents of Eu(III). However, almost simultaneously the formation of both the 1 : 2 and 1 : 1 stoichiometries also occurs. All of these species present in the solution until the end of the titration with the presence of the 1 : 1 complex in 58% yield, while the 1 : 2 and the 1 : 3 stoichiometry exist in 20% and 22% yield, respectively.
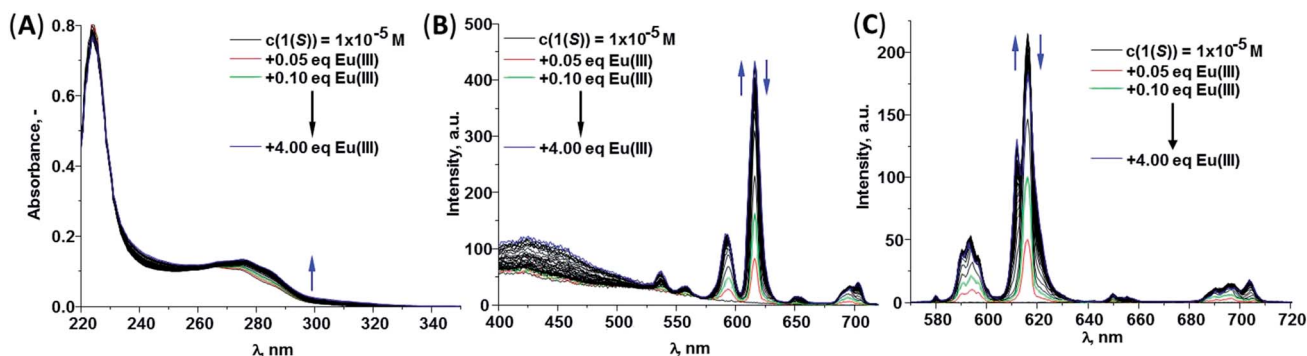

Fig. 4 The changes in the (A) absorption, (B) fluorescence and (C) Eu(III)-centred emission spectra of **1(S)** ($c = 1 \times 10^{-5}$ M) upon addition of $Eu(CF_3SO_3)_3$ in CH_3CN (25 °C, 0.05 M $(C_2H_5)_4NCl$).

Table 3 Binding constants obtained by fitting the changes in absorption, fluorescence and Eu(III)-centred emission spectra of **1(S)** or **1(R)** upon addition of Eu(CF$_3$SO$_3$)$_3$ in CH$_3$CN solution (25 °C, 0.05 M (C$_2$H$_5$)$_4$NCl)

Compound	Absorption			Fluorescence			Eu(III)-centred emission		
	$\log \beta_{1:1}$	$\log \beta_{1:2}$	$\log \beta_{1:3}$	$\log \beta_{1:1}$	$\log \beta_{1:2}$	$\log \beta_{1:3}$	$\log \beta_{1:1}$	$\log \beta_{1:2}$	$\log \beta_{1:3}$
1(S)	5.4 ± 0.3	11.1 ± 0.6	17.3 ± 0.4	6.2 ± 0.1	12.5 ± 0.2	17.9 ± 0.2	6.7 ± 0.2	—	17.4 ± 0.4
1(R)	5.7 ± 0.2	—	16.5 ± 0.5	6.2 (fix)	—	18.1 ± 0.2	6.9 ± 0.3	—	16.4 ± 0.4

The changes in the fluorescence emission and Eu(III)-centred emission were also monitored in parallel and are shown in Fig. 4B and C, respectively. The ligand fluorescence was weak and as such it was not possible to monitor the changes in the ligand-centred emission accurately over the cause of the titration. However, upon addition of the lanthanide to a solution of **1(S)** the formation of **Eu:L** assemblies between the two was clear from the appearance of the red Eu(III)-centred emission bands due to the deactivation of $^5D_0 \rightarrow {}^7F_J$ ($J = 0$–4) upon excitation of the ligand at 270 nm, Fig. 4B. Analysis of these fluorescence emission changes, showed that the luminescence intensity of the $^5D_0 \rightarrow {}^7F_{1,3,4}$ bands increased up until the addition of 0.30 equivalents of Eu(III), after which the emission plateau. In contrast, the changes in the $^5D_0 \rightarrow {}^7F_2$ based transition were more stepwise where an initial increase was observed upon addition of 0.30 equivalents of Eu(III), followed by slower increase in the intensity until the addition of 0.50 equivalents where the saturation of the luminescence intensity occurred.

Similar luminescence behaviour was observed in the Eu(III)-centred emission spectra by recording the delayed emission from the ion in phosphorescence mode. Here, the fine structure in the emission transitions was more pronounced as is evident from Fig. 4C, for the splitting of $^5D_0 \rightarrow {}^7F_2$ band into two maxima at 612 and 616 nm. The intensity of the band at 616 nm reaches its maximum upon addition of 0.30 equivalents of Eu(III) (Fig. 4C, see ESI†) while the intensity of the band at 612 nm increases gradually until the addition of 1.00 equivalent of Eu(III) after which the emission saturated (see ESI†). The presence of $^5D_0 \rightarrow {}^7F_0$ band suggests the formation of 1 : 3 species with the arrangement of the ligands around Eu(III) ion in C_3 symmetry confirming the results found in the crystal structure of **Eu(1(R))$_3$** complex (see above). Analysis of the changes in the Eu(III)-centred emission spectra confirmed the formation of the expected 1 : 1, 1 : 2 and 1 : 3 species in the solution.

The changes in both the fluorescence and the Eu(III)-centred emission spectra were analysed using non-linear regression analysis program SPECFIT®. As expected the factor analysis for the changes in the fluorescence emission spectra suggests the presence of four emissive species, while in the case of Eu(III)-centred emission three emissive species were identified. The changes were fitted to the same equilibrium used for analysis of the ground state data, showing similar binding constants as seen in Table 3.

Monitoring self-assembly formation between 1(S) or 1(R) and La(III) in CD$_3$CN solution by ^{1}H NMR spectroscopy

The interaction between the ligands and lanthanide ions in CD$_3$CN solution was also studied using NMR spectroscopy where the binding was monitored using diamagnetic lanthanum ions as ^{1}H NMR spectra of the Eu(III) complexes were too broadened and shifted to be fully analysed. The overall changes are seen in Fig. 6, where the ^{1}H NMR of the free ligand can be seen and assigned (*i.e.* Scheme 1 for assignment and ESI†).

The changes in ^{1}H NMR spectra of **1(S)** or **1(R)** were followed upon addition of La(CF$_3$SO$_3$)$_3$ and identical for both enantiomers (Fig. 6 and ESI†). This reflected the formation of a single species in solution on the NMR time-scale. Generally, upon addition of La(III) the NMR spectra became both broadened and shifted indicating complexes formed in the solution. More specifically, the CH(**2**) protons were shown to be shifted upfield, while N–H protons (NH(**13**)) were shifted downfield. Clear binding of the La(III) to the pyridine ring can be also confirmed by broadening of the proton resonances (CH(**10–12**)). Similarly the changes in the naphthyl group protons CH(**3,4**) occurred with very minor downfield shift while CH(**5–9**) experienced much more significant changes resulting in an upfield shift and appearance of the new resonances, which is indicative of the recognition process being in slow exchange. Thus, even though the exact mode of binding cannot be established it is possible to conclude that the binding of La(III) to **1(S)** or **1(R)** occurs through the pyridine centre with further rearrangement of the naphthyl groups around metal centre. The evolution of the changes in the spectra suggest the possible occurrence of 1 : 1, 1 : 2 and 1 : 3 (**M:L**) species.

Circular dichroism and circularly polarised luminescence spectroscopy studies

In our previous work,[8–12] we have used circular dichorsim and circularly polarised luminescence to demonstrate the chirality associated with the formation of lanthanide self-assemblies such as in "Trinity Sliotar" complexes, as well as triple stranded dimetallic lanthanide helicates. In these, the Eu(III) CPL emission was recorded, demonstrating that the complexes and helicates were formed as pairs of enantiomers, where the chirality of the ligands was transferred to the complexes, giving Δ and Λ absolute stereochemistry. Similarly, we set out to probe the chiral nature and enantiomeric purity of **1(S)** or **1(R)** and their Eu(III) complexes using CD along with CPL spectroscopy. The CD spectra of both ligands and their corresponding Eu(III) complexes were recorded in both CH$_3$OH and CH$_3$CN solvent systems at 1×10^{-5} M and are shown in Fig. 7. All the structures showed clear Cotton effects and the expected mirror images for each pair of ligands (*i.e.* demonstrating that **1(S)** or **1(R)** are synthesised as enantiomers) and complexes in both solvent
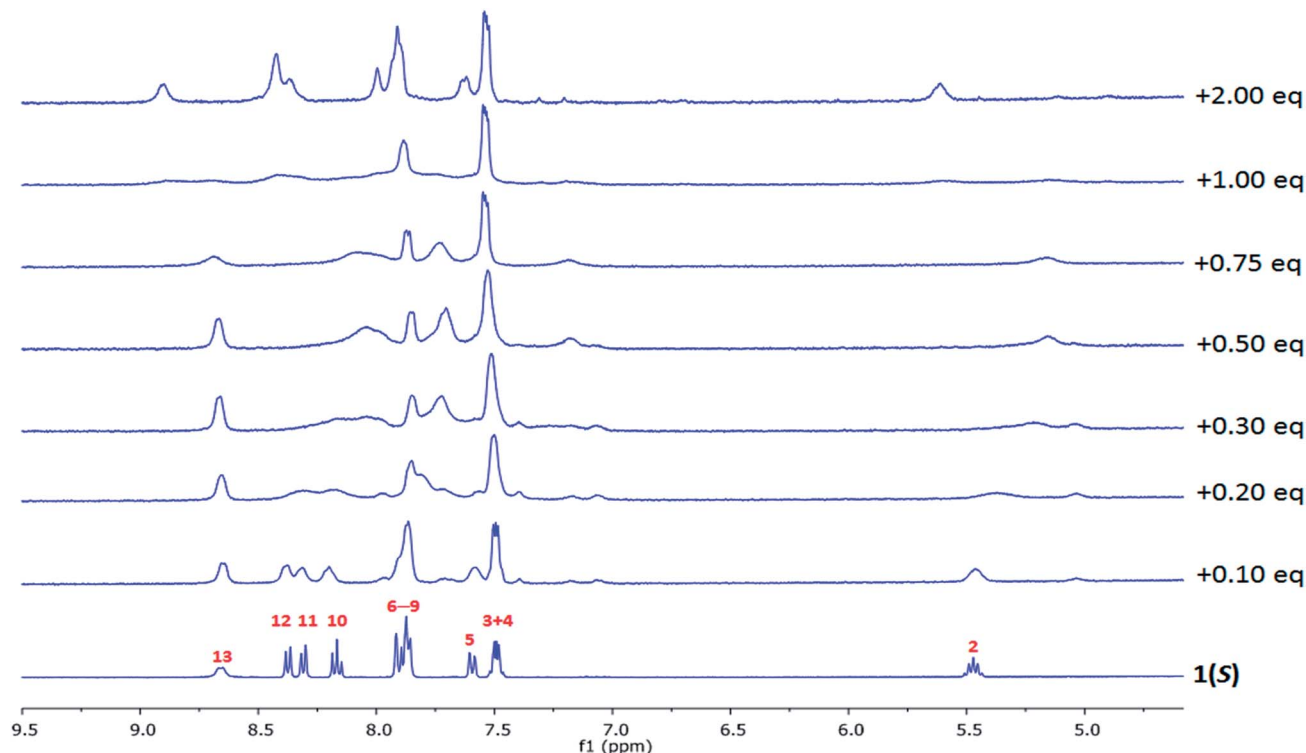
Fig. 6 The changes in the ^{1}H NMR spectra (400 MHz) of **1(S)** ($c = 4.26 \times 10^{-4}$ M) upon gradual addition of La(CF$_3$SO$_3$)$_3$ in CD$_3$CN.

systems. The fact that both **Eu(1(S))$_3$** and **Eu(1(R))$_3$** give rise to equal but opposite dichroism bands is consistent with the presence of a single chiral stereoisomer in solution for these two complexes. In both CH$_3$OH and CH$_3$CN the CD spectra of the ligands are very similar with the $\pi \rightarrow \pi^*$ transitions resulting in the signals of maxima 273, 231 and 221 nm with the only difference being the ellipticity of the signals Fig. 7, which is significantly different for the two solvent systems. This clearly demonstrates the role solvent plays herein. Moreover, the spectra of the ligands can be characterised by Davydov splitting of 11 and 42 nm and this was observed in both solvents.[14,23] The

CD spectra of **Eu(1(S))$_3$** and **Eu(1(R))$_3$** possess very different structure compared to the ones observed for their corresponding ligands. However, again the spectra of the complexes are very similar between CH$_3$OH and CH$_3$CN with the maxima at 283, 253 and 228 nm and Davydov splitting of 23 and 35 nm. It has to be noted that the ratio between the degrees of ellipticity for the maxima in the CD spectra of **EuL$_3$** (**L** = **1(S)**, **1(R)**) recorded in CH$_3$OH and CH$_3$CN are different which can be related to the solvent effect causing dissociation of **EuL$_3$** $\leftrightarrow$ **EuL$_2$** + **L** in presence of protic solvent. This was observed previously while recording the life-times of Eu(III)-centred

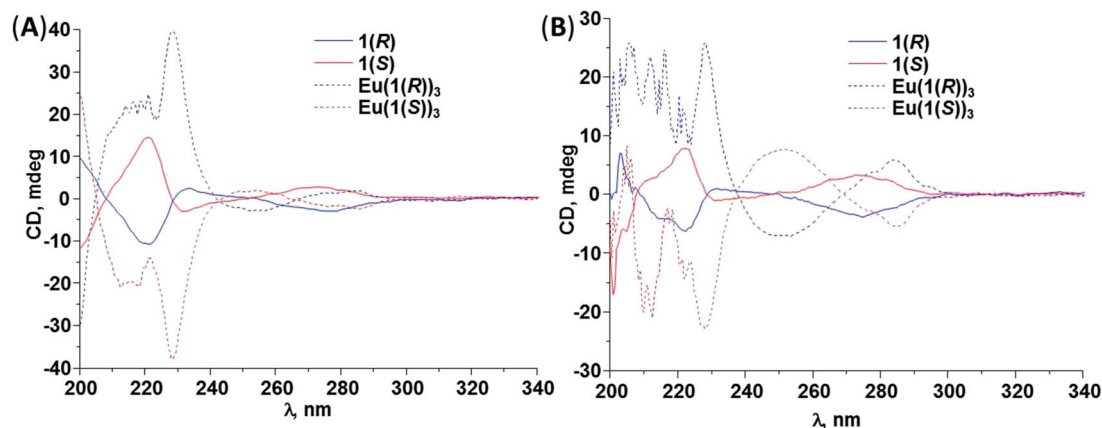**Fig. 7** CD spectra of **1(S)** (—) and **1(R)** (—) along with **Eu(1(S))$_3$** (—) and **Eu(1(R))$_3$** (—) recorded in (A) CH$_3$CN and (B) CH$_3$OH solvents at $c = 1 \times 10^{-5}$ M, 25 °C.

emission in CH$_3$OH, as summarised in Table 1. The presence of only **EuL$_3$** species in aprotic solvent at $c = 1 \times 10^{-5}$ M was confirmed by recording the Eu(III) ^{5}D$_0$ excited state life-times which were best fitted to monoexponential decay with $\tau \approx 1.99 \pm 0.06$ ms for both enantiomers.

The occurrence of bisignate intense CD Cotton effects suggests possible coupling between naphthyl chromophores as previously was observed by Parker *et al.* (exciton coupling).[24] In order to elucidate the effect of temperature on the interaction of the aromatic groups we recorded CD spectra of Eu(III) complexes in the temperature range varying from −10 to 60 °C. However, we did not observe an enhancement in the CD signals or a change in Davydov splitting (see ESI†), but the shape of CD spectra suggests the presence of the coupling interactions between aromatic antennas.

As stated above, CD spectroscopy has been widely used for performing quantitative analysis of various supramolecular systems, but mainly focusing on the interaction of biological substrates with organic molecules, hydrogen-bonded and salt-bridged complexes or chirality-sensing systems.[14,25] However, to the best of our knowledge, only very few reports study the self-assembly between organic ligands and Ln(III) ions in solution.[12b,26] Consequently, we studied the binding equilibrium processes of Eu(III) to both **1(S)** and **1(R)** ligands in CH$_3$CN solution by monitoring the changes in the main CD bands, following a titration of these ligands with Eu(III) as shown in Fig. 8A (see also ESI†). As the binding constants for **Eu:L$_n$** assemblies were previously determined in CH$_3$CN solution in presence of 0.05 M (C$_2$H$_5$)$_4$NCl, we monitored the changes in the same ionic media. It should be stated that the observed changes for one enantiomer are mirror images of the other and this can be clearly seen from the binding isotherms of the main bands *versus* equivalents of Eu(III) added into the solution, as shown in ESI†. In order to monitor conformational changes that can possibly occur in the solution the CD spectra were recorded directly after each addition and after 24 hours equilibration. However, in this particular case, no significant differences occurred upon equilibration. Similarly to our previous self-assembly studies the main changes in the spectra occur upon addition of 0 → 1 equivalents of Eu(III) to the solution and

indicates the formation of 1 : 1, 1 : 2 and 1 : 3 species. In order to perform more detailed analysis about the equilibria occurring in the solution here we attempted to fit the data obtained using non-linear regression analysis program SPECFIT® in a similar manner to that carried out for the changes in the ground state absorption and the emission above. For both of the enantiomers, the least square factor analysis of the titration results suggested the presence of four responding species in the CD spectra, which was in line with our previous findings discussed above. Based on our previous results and current data we anticipated the successive formation of 1 : 1, 1 : 2 and 1 : 3 species. Indeed, our analysis showed the formation of all of these species, which were comparable to those obtained by fitting the changes in the absorption and luminescence data. Hence, for example, in the case of **1(S)** binding constants of log $\beta_{1:1} = 6.6 \pm 0.5$, log $\beta_{1:2} = 12.8 \pm 0.6$ and log $\beta_{1:3} = 18.3 \pm 0.6$ were determined. Gratifyingly, the fitting of the titration of **1(R)** with Eu(III) gave almost indicial results (within experimental error) of log $\beta_{1:1} = 6.5 \pm 0.5$, log $\beta_{1:2} = 12.0 \pm 0.8$ and log $\beta_{1:3} = 18.7 \pm 0.6$. These binding constant results are slightly higher than determined above, but this can be attributed to the presence of (C$_2$H$_5$)$_4$NCl in the solution which did not allow monitoring the CD changes in the 200–223 nm spectral range and as such we were only able to analyse the changes in 275 and 226 nm bands, both of which possess small amplitude. It is clear from these results that the self-assembly processes can be both monitored and quantified, as well as that the results are comparable to that observed using more classical fitting of absorbance and emission data. Thus probing the chiroptical properties of the lanthanide directed self-assembly process in real time allows for additional information to be revealed that can help us in furthering quantification and revealing more understanding of such processes. As the overall changes in the circular dichroism spectra are quite significant they can also be employed as a fingerprint or signature for each of the stochiometries in solution. This is commonly done in the treatment of absorption spectra titrations data, where the information from the data fitting can also be employed to generate calculated spectra of each of the species in solution. The changes observed in the CD spectra of **1(S)** shown in Fig. 8A cannot be accurately
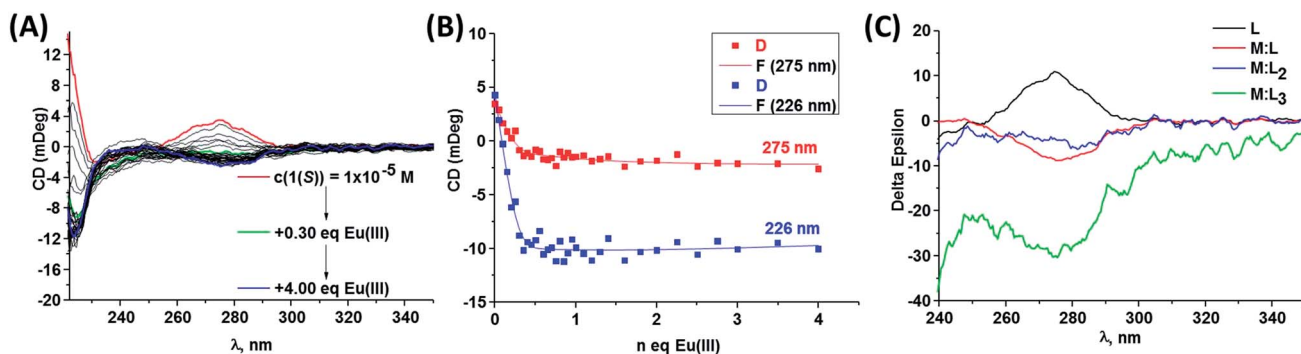

Fig. 8 (A) Changes in CD spectra of **1(S)** (−) ($c = 1 \times 10^{-5}$ M) upon addition of Eu(CF$_3$SO$_3$)$_3$, (B) experimental binding isotherms representing the changes in the CD bands upon gradual Eu(CF$_3$SO$_3$)$_3$ addition in CH$_3$CN (25 °C, 0.05 M (C$_2$H$_5$)$_4$NCl) and (C) recalculated CD spectra obtained with SPECFIT®.

presented as a 'signature' for each of the three stochiometries. In comparison, the calculated spectra generated for the changes in the CD titrations in CH_3CN are shown in Fig. 8C for $\mathbf{1(S)}$ and these clearly demonstrate that each of the species can be assigned. For example, the experimental CD spectrum of $\mathbf{Eu(1(S))_3}$ (Fig. 7A) shows negative band centred at 273 nm similarly to the one observed for the calculated spectrum (Fig. 8C). Each of these calculated spectra can, therefore, be employed as a fingerprint, or a signature, for that given species. This again, demonstrates the potential use of CD spectroscopy in accessing vital information about equilibrium processes in metal directed synthesis of supramolecular structures.

Having emissive metal centre in a chiral environment we further investigated the chiroptical properties of our systems using CPL spectroscopy. As anticipated the excitation into the ligand absorption bands resulted in energy transfer to Eu(III) ion and thus generation of mirror-image CPL spectra showing the appearance of $^5D_0 \rightarrow {}^7F_J$ ($J = 0–4$) transition bands, as shown in Fig. 9. The luminescence dissymmetry factors g_{lum}, were calculated for all of these transitions (see ESI†) and for $^5D_0 \rightarrow {}^7F_1$ (589 nm) were found to be 0.16 and −0.15, while for $^5D_0 \rightarrow {}^7F_2$ (614 nm) these values were equal to −0.09 for the Eu(III) complex with $\mathbf{1(S)}$ and 0.10 for $\mathbf{1(R)}$, respectively. These correspond well to values that we previously obtained for similar asymmetrical complexes with 1-naphthyl antennae complexes[11] reflecting the similarities in the helical twists, nature of the ligand field, donor group solvation and time-averaged local helicity around Eu(III) of $\mathbf{Eu(1(S))_3}$ and $\mathbf{Eu(1(R))_3}$. The values for Eu(III) complexes with asymmetrical ligands are lower than these obtained in our group previously[7,8,9b] as well as these obtained by Muller *et al.*[4c] for the complexes with symmetrical ligands. However, this can be simply explained by the decrease in the degree of conformational rigidity of the complex when reducing the symmetry of the ligand. Overall, obtained g_{lum} values are high as enantiopure Eu(III) and Tb(III) complexes typically possess these values between 0.1 and 0.5 and much higher compared to the chiral fluorescent organic molecules where $g_{lum} < 0.01$.[3a,b]
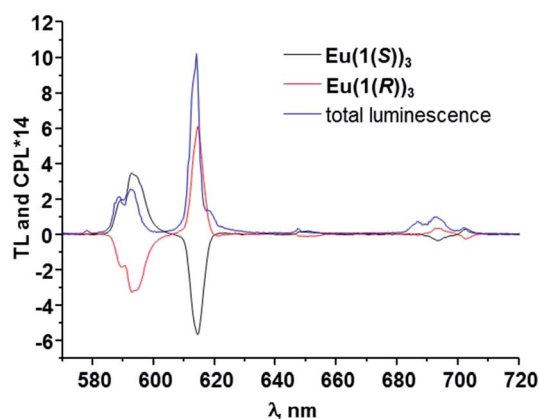

Fig. 9 The CPL spectra for EuL$_3$ in CH_3OH (L = $\mathbf{1(S)}$, $\mathbf{1(R)}$). The total luminescence is also shown.

Based on our previous work,[7,8,9b] where we have assigned the absolute configuration of lanthanide based self-assembly complexes and helices, formed from chiral ligands with known absolute stereochemistry, as Δ or Λ, then from the circularly polarised emission in Fig. 9, we were able to do the same for $\mathbf{Eu(1(S))_3}$ and $\mathbf{Eu(1(R))_3}$ by comparison. The CPL spectra of both $\mathbf{Eu(1(S))_3}$ and $\mathbf{Eu(1(R))_3}$ were structurally identical to that observed for "Trinity Sliotar" complexes. Hence, the CPL of $\mathbf{Eu(1(R))_3}$ consists of a negative CPL signal for the $\Delta J = 1$, a positive band for the $\Delta J = 2$, and a split CPL signal for the $\Delta J = 4$ (into a positive and a negative band), and these are identical not only in their sign, but also in the intensity ratio to that seen for the *RR* isomer used in the synthesis of the Λ "Trinity Sliotar" complex.[7,8] Similarly, the *RR* isomer used in the formation of structurally similar dimetallic Eu(III) triple stranded helicates,[9b] gave also such identical CPL spectra. Consequently, we can with a degree of confidence, assign the absolute stereochemistry of $\mathbf{Eu(1(R))_3}$ as Λ; and consequently the absolute stereochemistry of the $\mathbf{Eu(1(S))_3}$ complex as Δ. Moreover, we were able to assign the configuration of $\mathbf{Eu(1(R))_3}$ with absolute certainty since we have grown its crystals of good enough quality for crystallographic determination (see above) and as such clearly relate spectroscopical data to known solid state structures of several "Trinity Sliotar" complexes resolved in our laboratory.

Conclusions

Chiral asymmetrical *R*- and *S*- 6-(1-(naphthalen-2-yl)ethyl-carbamoyl)pyridine-2-carboxylic acids ($\mathbf{1(S)}$ and $\mathbf{1(R)}$) were obtained in three steps and high yield. These ligands were reacted with Eu(III) ions resulting in the formation of red emissive complexes, of $\mathbf{Eu(1(S))_3}$ and $\mathbf{Eu(1(R))_3}$, respectively, with ~2% luminescence quantum yields in CH_3CN solution. Crystal structures of $\mathbf{1(S)}$ and $\mathbf{1(R)}$ along with their benzyl protected forms ($\mathbf{4(S)}$ and $\mathbf{4(R)}$) were obtained from $CH_3CN–CH_3OH$ or CH_3OH solvent systems and all crystallized in the chiral space group $P2_1$, while $\mathbf{Eu(1(R))_3}$ crystallized in an orthorhombic crystal system with chiral space group $C222_1$. The self-assembly formation between $\mathbf{1(S)}$ and $\mathbf{1(R)}$ with $Eu(CF_3SO_3)_3$ in aprotic CH_3CN polar media were analysed using ^1H NMR, absorption, luminescence and CD spectroscopies at room temperature. In all the cases the changes suggests successive formation of $\mathbf{M:L}$, $\mathbf{M:L_2}$ and $\mathbf{M:L_3}$ assemblies with comparable values of the binding constants. As expected the excitation into the ligands absorption bands resulted in the transfer of the chirality from the ligand onto the metal centres showing characteristic Eu(III) CPL bands. This allowed us to tentatively assign the absolute stereochemistry of the self-assemblies as Δ and Λ for $\mathbf{Eu(1(S))_3}$ and $\mathbf{Eu(1(R))_3}$, respectively, and absolutely confirm it for $\mathbf{Eu(1(R))_3}$ by comparing to the solid state crystallographic data obtained. Here, we represent one of the rare examples where the binding constants of supramolecular self-assemblies were determined by fitting the changes in the chiroptical spectra (CD) using non-linear regression analysis. This allowed us to identify three species in solution as the 1 : 1, 1 : 2 and 1 : 3 metal to ligand stoichiometries and quantify their binding constants, all of which gave good correlation with those

determined by fitting the changes in the absorption and luminescence spectra. Moreover, the analysis of the CD spectra of the ligands and their Eu(III) complexes allowed us to suggest the presence of exciton coupling between the aromatic chromophores in these assemblies. Furthermore, using the information of the fitting of the CD data, allowed us to calculate the CD spectra of each of the three stoichiometries, which we can use as fingerprints or signatures for each one. We are actively employing CD spectroscopy in greater detail for the analysis of metal-directed synthesis of supramolecular structures.

Experimental

Materials and methods

All solvents and chemicals were purchased from commercial sources and used without further purification. Dichloromethane and methanol were freshly distilled under argon atmosphere prior to use. Water was purified using a Millipore Milli-Q water purification system (18.2 MΩ cm). Hydrochloric acid, sodium bicarbonate, Na_2SO_4, $MgSO_4$, **H₂dpa**, benzyl bromide, HOBt, triethylamine (Et₃N), triethylsilane (Et₃SiH), palladium on carbon (10 wt% loading), tetraethylammonium chloride ((C_2H_5)₄NCl), Eu(CF₃SO₃)₃·6H₂O were purchased from Sigma-Aldrich, while N,N-dimethylformamide, (S)- or (R)-1-(1-naphthyl)-ethylamine and (S)- or (R)-1-(2-naphthyl)-ethylamine and EDCI·HCl from TCI Europe. Deuterated solvents used for NMR analysis (CDCl₃, CD₃OD, (CD₃)₂SO) were purchased from Apollo Scientific. The ¹H NMR spectra were recorded at 400 MHz using an Agilent Technologies 400-MR NMR Spectrometer. The ¹³C NMR spectra were recorded at 100 MHz using an Agilent Technologies 400-MR NMR Spectrometer. NMR spectra were also recorded using a Bruker AV-600 instrument operating at 600.1 MHz for ¹H NMR and 150.9 MHz for ¹³C NMR. ¹H NMR titrations were recorded using Bruker Spectrospin DPX-400 instrument operating at 400.1 MHz. The titrations for both enantiomers were started with the ligands at $c = 4.26 \times 10^{-4}$ M upon gradual addition of La(CF₃SO₃)₃ solution in CD₃CN. Chemical shifts are reported in ppm with the deuterated solvent as the internal reference. All NMR spectra were carried out at 293 K. Mass-spectrometry was carried out using HPLC grade solvents. Electrospray mass spectra were determined on a Micromass LCT spectrometer and high resolution mass spectra were determined relative to a standard of leucine enkephaline. Maldi-Q-Tof mass spectra were carried out on a MALDI-Q-TOF-Premier (Waters Corporation, Micromass MS technologies, Manchester, UK) and high resolution mass spectrometry was performed using Glu-Fib with an internal reference peak of m/z 1570.6774. Melting points were determined using an Electrothermal IA9000 digital melting point apparatus. Infrared spectra were recorded on a Perkin Elmer Spectrun One FT-IE spectrometer equipped with universal ATR sampling accessory. Elemental analysis was conducted at the Microanalytical Laboratory, School of Chemistry and Chemical Biology, University College Dublin.

Complexation reactions were carried out in 2–5 mL Biotage Microwave Vials in a Biotage Initiator Eight EXP microwave reactor.

Crystallographic experimental section

Diffraction data for all compounds were collected on a Bruker APEX 2 DUO CCD diffractometer using graphite-monochromatized Mo-Kα ($\lambda = 0.71073$ Å) and Incoatec IµS Cu-Kα ($\lambda = 1.54178$ Å) radiation. Crystals were mounted in a cryoloop/MiTeGen micromount and collected at 100(2) K using an Oxford Cryosystems Cobra low temperature device. Data were collected using omega and phi scans and were corrected for Lorentz and polarization effects.[27a]

The structures **1(R)**, **1(S)**, **4(R)** and **4(S)** were solved by direct methods and refined by full-matrix least-squares procedures on F^2 using SHELXL-2013 software.[27b] All non-hydrogen atoms were refined anisotropically. Hydrogen atoms were added geometrically in calculated positions and refined using a riding model.

The structure for complex **Eu(1(R))₃** was solved initially using SHELXS-97 which was further refined using SHELXL-97. Some of the aromatic moieties which showed high disorder were constrained to regular geometry. Low resolution and low data/parameter ratio prevented in some cases full anisotropic refinement. The thermal parameters were either restrained or refined isotropically. Hydrogen atoms were placed geometrically using suitable constraints except for water molecules in which case they were placed to form a coherent hydrogen bond network and their positions kept fixed.

Details of the data collection and refinement are given in Table 1.†

Photophysical measurements

Unless otherwise stated, all measurements were performed at 298 K in acetonitrile solutions (spectroscopy grade, Aldrich). UV-visible absorption spectra were measured in 1 cm quartz cuvettes on a Varian Cary 50 spectrophotometer. Baseline correction was applied for all spectra. Emission (fluorescence, phosphorescence and excitation) spectra and life-times were recorded on a Varian Cary Eclipse Fluorimeter. Quartz cells with a 1 cm path length from Hellma were used for these measurements. The temperature was kept constant throughout the measurements at 298 K by using a thermostated unit block. Phosphorescence life-times of the Eu($^5D_0$) excited state were measured in both water/deuterated water solutions in time-resolved mode at 298 K. They are averages of three independent measurements, which were made by monitoring the emission decay at 616 nm, which corresponds to the maxima of the Eu(III) $^5D_0 \rightarrow {}^7F_2$ transition, enforcing a 0.1 ms delay, and were analyzed using Origin 7.5®. The number of water molecules directly bonded to Eu(III) center (q value) was determined according to the equation developed by Parker et al.:[17]

$$q = A(\tau_{O-H}^{-1} - \tau_{O-D}^{-1}) \tag{1}$$

where τ_{O-H} is the life-time water or methanol solutions, τ_{O-D} is the life-time measured in deuterated water or deuterated methanol solutions.

The quantum yields ($Q_{rel}^{Eu,L}$) were measured by relative method[28,29] using Cs₃[Eu(**dpa**)₃]·9H₂O complex in 0.1 M Tris buffer (pH = 7.45) ($Q_{abs}^{Eu} = 24.0 \pm 2.5\%$)[19] as a standard with

known quantum yield, to which the absorbance and emission intensity of the sample are compared according to:

$$Q_{rel}^{Eu,L} = \frac{Q_x}{Q_r} = \frac{E_x}{E_r} \times \frac{A_r(\lambda_r)}{A_x(\lambda_x)} \times \frac{I_r(\lambda_r)}{I_x(\lambda_x)} \times \frac{n_x^2}{n_r^2} \qquad (2)$$

where subscript r – reference and x – sample; E – integrated luminescence intensity; A – absorbance at the excitation wavelength; I – intensity of the excitation light at the same wavelength, n – refractive index of the solution. The estimated error for quantum yields is ±10%.

τ_R life-time was obtained using eqn (3):

$$\frac{1}{\tau_R} = A_{MD,0} n^3 \left(\frac{I_{tot}}{I_{MD}} \right) \qquad (3)$$

where n is the refractive index of the solvent, $A_{MD,0}$ is the spontaneous emission probability for the $^5D_0 \rightarrow {}^7F_1$ transition *in vacuo*, and I_{tot}/I_{MD} is the ratio of the total area of the corrected Eu(III) emission spectrum to the area of the $^5D_0 \rightarrow {}^7F_1$ band ($A_{MD,0} = 14.65 \text{ s}^{-1}$).[30]

The quantum yield of the luminescence step (Φ_{Ln}^{Ln}) expresses how well the radiative process complete with non-radiative processes.

$$\Phi_{Ln}^{Ln} = \frac{\tau_{obs}}{\tau_R} \qquad (4)$$

The efficiency of lanthanide sensitization (η_{sens}) is the ratio between Φ_{tot} (determined experimentally) and Φ_{Ln}^{Ln} (see eqn (4)):

$$\eta_{sens} = \frac{\Phi_{tot}}{\Phi_{Ln}^{Ln}} \qquad (5)$$

CD spectra were recorded in both acetonitrile and methanol solutions on a Jasco J-810-150S spectropolarimeter. CD titrations were performed in CH_3CN media starting with the ligands at $c = 1 \times 10^{-5}$ M upon gradual addition from 0 to 4 equivalents of $Eu(CF_3SO_3)_3$ to the solution. CPL spectra were recorded by Dr R. Peacock at the University of Glasgow. Excitation of Eu(III) (560–581 nm) was accomplished by using a Coherent 599 tunable dye laser (0.03 nm resolution) with argon ion laser as a pump source. Calibration of the emission monochromator was accomplished by passing scattered light from a low power HeNe laser through the detection system. The optical detection system consisted of a photoelastic modulator (PEM, Hinds Int.) operating at 50 kHz and a linear polarizer, which together act as a circular analyzer, followed by a long pass filter, focusing lens and a 0.22 m double monochromator. The emitted light was detected by a cooled EM1-9558QB photomultiplier tube operating in photon counting mode. The 50 kHz reference signal from the photoelastic modulator was used to direct the incoming pulses into two separated counters. An up counter, which counts every photon pulse and thus is a measure of the total luminescence signal $I = I_{left} + I_{right}$, and an up/down counter, which adds pulses when the analyzer is transmitting to the left circularly polarized light and subtracts pulses when the analyzer is transmitting right circularly polarized light. The second counter provides a measure of the differential emission intensity $\Delta I = I_{left} - I_{right}$.

Spectrophotometric titrations and binding constants

The formation of the luminescent 1 : 1, 1 : 2 and 1 : 3 (**M:L**, where **M** = Eu(III) and **L** = **1(S)**, **1(R)**) species was ascertained by both UV-visible, luminescence and CD titrations of a solution of **L** (1×10^{-5} M) in CH_3CN in presence of 0.05 M $(C_2H_5)_4NCl$ with $Eu(CF_3SO_3)_3 \cdot 6H_2O$ ($0 \rightarrow 4$ equivalents). The data were fitted using the non-linear regression analysis program, SPECFIT®.[21]

Synthesis of 6-((benzyloxy)carbonyl)pyridine-2-carboxylic acid (2)

Compound **2** was synthesised by stirring 2,6-pyridinedicarboxylic acid (**H₂dpa**; 6.00 g, 3.59×10^{-2} mol, 1 equivalent) with $NaHCO_3$ (3.62 g, 4.31×10^{-2} mol, 1.2 equivalents) in N,N-dimethylformamide solution (100 mL) at 60 °C under argon for 30 minutes. Benzyl bromide (5 mL, 4.31×10^{-2} mol, 1.2 equivalents) was then added to this white suspension and left to stir under argon at 60 °C overnight. Resulting clear yellow solution was diluted with water and neutralised with saturated solution of $NaHCO_3$ (pH ~ 8) and extracted with diethyl ether to remove diester side product. The aqueous layer was acidified with 2 M HCl and extracted with ethyl acetate. Then, the organic layer was dried over Na_2SO_4, filtered and after the solvent was evaporated the resulting solid was solubilised in dichloromethane. This solution was washed with water and brine (3 × 20 mL) after which the organic layer was dried over $MgSO_4$, filtered and after subsequent evaporation of the solvent white powder was obtained (3.47 g, 38% yield). M.p. 138 °C; HRMS (m/z) (ES⁻) calculated for $C_{14}H_{10}NO_4$ $m/z = 256.0610$ [M − H]⁻. Found $m/z = 256.0613$; ¹H NMR (400 MHz, CDCl₃, δ_H) ppm 8.39 (q, $J = 8.40$ Hz, 2H, CH_{py}), 8.11 (t, $J = 8.10$ Hz, 1H, CH_{py}), 7.49–7.47 (m, 2H, CH_{ph}), 7.44–7.36 (m, 3H, CH_{ph}), 5.46 (s, 2H, CH_2); ¹³C NMR (150 MHz, CDCl₃, δ_C) 163.46, 163.39, 146.72, 139.62, 134.96, 128.85, 128.77, 128.59, 126.85, 68.07; IR ν_{max} (cm⁻¹): 3064, 2879, 2560, 1736, 1695, 1609, 1466, 1416, 1376, 1328, 1289, 1244, 1152, 1005, 994, 956, 940, 855, 796, 784, 754, 728, 710, 648; anal. calc. for $C_{14}H_{11}NO_4$, %: C 65.4, H 4.3, N 5.4; found, %: C 65.1, H 4.2, N 5.3.

Preparation of 4(S) and 4(R)

General procedure. To a stirred solution of (S or R)-2-(1-aminoethyl)naphthalene (**3(S)** or **3(R)**, 1.0 equivalent) in 30 mL of freshly distilled dichloromethane, HOBt (1.0 equivalent) and 6-((benzyloxy)carbonyl)pyridine-2-carboxylic acid (**2**, 1.0 equivalent) were added. The solution was stirred for 30 minutes at 0 °C under an inert atmosphere of argon before the solution of 1-(3-dimethylaminopropyl)-3-ethylcarbodiimide hydrochloride (EDCI·HCl, 1.1 equivalents) and triethylamine (1.1 equivalents) in 30 mL of dichloromethane was added dropwise. The reaction mixture was then stirred for further 30 minutes at 0 °C under argon atmosphere, then allowed to reach room temperature and left stirring for 48 hours. The insoluble residue was removed by suction filtration before reaction mixture was washed with 1 M HCl, a saturated solution of $NaHCO_3$, and water (each 2 × 20 mL). The organic layer was then dried over $MgSO_4$, filtered, and the solvent removed

under reduced pressure. The obtained yellow-white powders where purified using normal phase silica column chromatography eluting with 95% dichloromethane and 5% methanol ($R_f = 0.9$).

(S)-6-(1-(Naphthalen-2-yl)ethylcarbamoyl)pyridine-2-carboxylate (4(S)). Compound 4(S) was synthesized by stirring solution of (S)-1-(2-naphthyl)-ethylamine (3(S), 0.67 g, 3.9×10^{-3} mol) in 30 mL of freshly distilled dichloromethane, HOBt (0.53 g, 3.9×10^{-3} mol) and 6-((benzyloxy)carbonyl)pyridine-2-carboxylic acid (2, 1.00 g, 3.9×10^{-3} mol) for 30 minutes at 0 °C under an inert atmosphere of argon before EDCI·HCl (0.79 g, 4.1×10^{-3} mol) and triethylamine (0.73 mL, 4.1×10^{-3} M) were then added dropwise according to the general procedure. The obtained light yellow powder was purified using normal phase silica chromatography using 95% dichloromethane–5% methanol solvent mixture as eluent ($R_f = 0.9$, 1.23 g, 78% yield). M.p. 130 °C; HRMS (m/z) (ES$^+$) calculated for $C_{26}H_{22}N_2O_3Na$ $m/z = 433.1528$ [M + Na]$^+$. Found $m/z = 433.1548$; ^{1}H NMR (400 MHz, CDCl$_3$, δ_H) ppm 8.50 (d, $J = 8.50$ Hz, 1H, NH), 8.39 (d, $J = 8.38$ Hz, 1H, CH), 8.23 (d, $J = 8.23$ Hz, 1H, CH), 7.99 (t, $J = 8.00$ Hz, 1H, CH), 7.85–7.81 (m, 4H, CH), 7.53 (d, $J = 7.52$ Hz, 1H, CH), 7.47 (m, 4H, CH), 7.34 (m, 3H, CH), 5.50 (t, $J = 5.52$ Hz, 1H, CH), 5.44 (s, 2H, CH_2), 1.72 (d, $J = 6.92$ Hz, 3H, CH_3); ^{13}C NMR (100 MHz, CDCl$_3$, δ_C) 164.34, 162.76, 150.31, 146.67, 140.58, 138.64, 135.55, 133.50, 132.89, 128.78, 128.68, 128.61, 128.34, 128.10, 127.73, 127.44, 126.30, 125.98, 125.60, 124.80, 124.78, 67.64, 49.27, 22.11; IR ν_{max} (cm^{-1}): 3396, 3060, 1732, 1680, 1588, 1504, 1452, 1439, 1381, 1283, 1229, 1182, 1165, 1151, 1083, 991, 959, 928, 897, 862, 770, 714, 689, 663, 649; anal. calc. for $C_{26}H_{22}N_2O_3$, %: C 76.1, H 5.4, N 6.8; found, %: C 75.9, H 5.3, N 6.7.

Benzyl-(R)-6-(1-(naphthalen-2-yl)ethylcarbamoyl)pyridine-2-carboxylate (4(R)). Compound 4(R) was synthesized by stirring solution of (R)-1-(2-naphthyl)-ethylamine (3(R), 0.67 g, 3.9×10^{-3} mol) in 30 mL of freshly distilled dichloromethane, HOBt (0.53 g, 3.9×10^{-3} mol) and 6-((benzyloxy)carbonyl)pyridine-2-carboxylic acid (2, 1.00 g, 3.9×10^{-3} mol) for 30 minutes at 0 °C under an inert atmosphere of argon before EDCI·HCl (0.79 g, 4.1×10^{-3} mol) and triethylamine (0.73 mL, 4.1×10^{-3} M) were then added dropwise according to the general procedure. The obtained light yellow powder was purified using normal phase silica chromatography using 95% dichloromethane–5% methanol solvent mixture as eluent ($R_f = 0.9$, 1.30 g, 81% yield). M.p. 130 °C; HRMS (m/z) (ES$^+$) calculated for $C_{26}H_{22}N_2O_3Na$ $m/z = 433.1528$ [M + Na]$^+$. Found $m/z = 433.1529$; ^{1}H NMR (400 MHz, CDCl$_3$, δ_H) ppm 8.50 (d, $J = 8.50$ Hz, 1H, NH), 8.39 (d, $J = 8.39$ Hz, 1H, CH), 8.23 (d, $J = 8.23$ Hz, 1H, CH), 7.99 (t, $J = 8.00$ Hz, 1H, CH), 7.85–7.80 (m, 4H, CH), 7.53 (d, $J = 7.53$ Hz, 1H, CH), 7.47 (m, 4H, CH), 7.34 (m, 3H, CH), 5.50 (t, $J = 5.50$ Hz, 1H, CH), 5.44 (s, 2H, CH_2), 1.72 (d, $J = 7.04$ Hz, 3H, CH_3); ^{13}C NMR (100 MHz, CDCl$_3$, δ_C) 164.37, 162.78, 150.34, 146.69, 140.60, 138.66, 135.56, 133.52, 132.91, 128.80, 128.69, 128.63, 128.35, 128.12, 127.74, 127.45, 126.31, 125.99, 125.63, 124.82, 124.79, 67.66, 49.29, 22.13; IR ν_{max} (cm^{-1}): 3396, 1732, 1681, 1588, 1501, 1453, 1439, 1381, 1282, 1229, 1165, 1151, 1084, 991, 959, 897, 862, 842, 815, 749, 731, 689, 662, 649; anal. calc. for $C_{26}H_{22}N_2O_3$, %: C 76.1, H 5.4, N 6.8; found, %: C 75.8, H 5.4, N 6.5.

Preparation of 1(S) and 1(R)[16]

General procedure. To a stirred solution of 4(S) or 4(R) (1 equivalent) and 10 wt% Pd–C (10–20% by weight) in methanol was added neat triethylsilane (20 equivalents) dropwise from a pressure-equalizing dropping funnel under an argon-filled balloon. The completion of the reaction was monitored using neutral phase silica TLC plates (95% dichloromethane–5% methanol). After the reaction was complete the solvent was evaporated and resulting oily product was taken into saturated solution of NaHCO$_3$. The aqueous layer was washed with diethyl ether in order to remove possible residue of starting material and triethylsilane and acidified using 2 M HCl until pH ~ 2 when a white precipitate occurred in the solution. The solid product was washed out of the aqueous layer with ethyl acetate which was then dried over Na$_2$SO$_4$ and filtered. The solvent was then evaporated under reduced pressure yielding the product as white polycrystalline precipitate.

(S)-6-(1-(Naphthalen-2-yl)ethylcarbamoyl)pyridine-2-carboxylic acid (1(S)). Triethylsilane (5.23 mL, 3.27×10^{-2} mol, 20 equivalents) solution in 10 mL of methanol was added dropwise to the solution of 4(S) (0.67 g, 1.64×10^{-3} mol, 1 equivalent) and 10 wt% Pd–C (0.13 g) in 20 mL of methanol. After the workup described in the general procedure white crystalline powder was obtained (0.40 g, 77% yield). M.p. 115 °C; HRMS (m/z) (ES$^-$) calculated for $C_{19}H_{15}N_2O_3$ $m/z = 319.1083$ [M − H]$^-$. Found $m/z = 319.1075$; ^{1}H NMR (600 MHz, CD$_3$OD, δ_H) ppm 8.32 (d, $J = 8.32$ Hz, 2H, CH_{py}), 8.16 (t, $J = 8.17$ Hz, 1H, CH_{py}), 7.89 (s, 1H, CH_{naph}), 7.83 (m, 3H, CH_{naph}), 7.58 (dd, $^3J_{H-H} = 7.58$ Hz, $^4J_{H-H} = 7.59$ Hz, 1H, CH_{naph}), 7.44 (m, 2H, CH_{naph}), 5.44 (q, $J = 5.46$ Hz, 1H, CH), 1.73 (d, $J = 7.04$ Hz, 3H, CH_3); ^{13}C NMR (150 MHz, CD$_3$OD, δ_C) 167.89, 164.89, 151.39, 148.35, 142.61, 140.58, 134.84, 134.06, 129.32, 128.91, 128.60, 128.57, 127.15, 126.84, 126.78, 125.86, 125.64, 50.73, 22.09; IR ν_{max} (cm^{-1}): 3291, 3058, 2978, 2930, 1732, 1654, 1527, 1451, 1347, 1243, 1180, 999, 952, 856, 818, 745, 681; anal. calc. for $C_{19}H_{10}N_2O_3 \cdot 0.1CH_2Cl_2$, %: C 69.8, H 4.9, N 8.5; found, %: C 69.9, H 4.8, N 8.4.

(R)-6-(1-(Naphthalen-2-yl)ethylcarbamoyl)pyridine-2-carboxylic acid (1(R)). Triethylsilane (7.78 mL, 4.87×10^{-2} mol, 20 equivalents) solution in 10 mL of methanol was added dropwise to the solution of 4(R) (1.0 g, 2.44×10^{-3} mol, 1 equivalent) and 10 wt% Pd–C (0.2 g) in 20 mL of methanol. After the workup described in the general procedure white crystalline powder was obtained (0.62 g, 80% yield). M.p. 115 °C; HRMS (m/z) (ES$^-$) calculated for $C_{19}H_{15}N_2O_3$ $m/z = 319.1083$ [M − H]$^-$. Found $m/z = 319.1080$; ^{1}H NMR (600 MHz, CD$_3$OD, δ_H) ppm 8.32 (dd, $^3J_{H-H} = 8.32$ Hz, $^4J_{H-H} = 8.33$ Hz, 2H, CH_{py}), 8.15 (t, $J = 8.16$ Hz, 1H, CH_{py}), 7.88 (s, 1H, CH_{naph}), 7.82 (m, 3H, CH_{naph}), 7.58 (dd, $^3J_{H-H} = 7.58$ Hz, $^4J_{H-H} = 7.59$ Hz, 1H, CH_{naph}), 7.44 (m, 2H, CH_{naph}), 5.45 (q, $J = 5.46$ Hz, 1H, CH), 1.72 (d, $J = 7.06$ Hz, 3H, CH_3); ^{13}C NMR (150 MHz, CD$_3$OD, δ_C) 167.66, 164.93, 151.43, 148.06, 142.39, 140.54, 134.91, 134.21, 129.32, 128.90, 128.60, 128.58, 127.15, 126.87, 126.78, 125.85, 125.64, 50.73, 22.14; IR ν_{max} (cm^{-1}): 3285, 3062, 2980, 2933, 1751, 1650, 1524, 1451, 1334, 1252, 1184, 952, 892, 847, 817, 743, 678, 642; anal. calc. for $C_{19}H_{10}N_2O_3 \cdot 0.1CH_2Cl_2$, %: C 69.8, H 4.9, N 8.5; found, %: C 69.9, H 4.7, N 8.4.

General synthesis of europium complexes

Eu(III) complexes were prepared by refluxing, under microwave radiation, the relevant ligand with $Eu(CF_3SO_3)_3 \cdot 6H_2O$ (0.33 equiv.) in acetonitrile (15 mL) for 30 minutes. The solution was subsequently cooled to room temperature and then precipitated by slow evaporation of the solvent at ambient conditions. The resulting white solid was filtered off and dried under vacuum.

Synthesis of Eu(1(S))₃. This complex was synthesized according to general procedure using ligand **1(S)** (0.060 g, 1.83 × 10⁻⁴ mol) and $Eu(CF_3SO_3)_3 \cdot 6H_2O$ (0.037 g, 6.10 × 10⁻⁵ mol). A white solid was obtained (0.035 g, 36.7% yield). Compound decomposed within 140–160 °C; HRMS (m/z) (MALDI-MS⁺) calculated for $C_{57}H_{45}N_6O_9EuK$ $m/z = 1147.2084$ [Eu(**1(S)**–H⁺)₃ + K⁺]⁺; found $m/z = 1147.2034$; ¹H NMR (600 MHz, CD₃CN, δ_H) ppm 9.19, 8.67, 8.54, 8.30, 8.19, 8.07, 7.87, 7.57, 7.50, 7.33, 7.25, 7.09, 5.43, 5.29, 4.69, 4.56, 4.32, 3.96, 3.50, 3.05, 2.94, 2.73, 1.70, 1.27, 0.88, 0.43, 0.14, −0.10, −0.75; IR ν_{max} (cm⁻¹): 3271, 3105, 1626, 1592, 1560, 1451, 1353, 1279, 1241, 1160, 1092, 1028, 905, 860, 820, 751, 707, 661, 635, 570, 547, 532, 523; anal. calc. for 1.0 [$EuC_{60}H_{48}F_9N_6O_{18}S_3$]·1.3[$EuC_{57}H_{45}N_6O_9$] ([**Eu(1(S))₃(CF₃SO₃)₃**]· **1.3[Eu(1(S)–H)₃]**), %: C 53.8, H 3.2, N 6.4, S 3.2; found, %: C 53.6, H 3.6, N 6.4, S 3.2.

Synthesis of Eu(1(R))₃. This complex was synthesized according to general procedure using ligand **1(R)** (0.061 g, 1.86 × 10⁻⁴ mol) and $Eu(CF_3SO_3)_3 \cdot 6H_2O$ (0.04 g, 6.18 × 10⁻⁵ mol). A white solid was obtained (0.032 g, 33.3% yield). Compound decomposed within 140–160 °C; HRMS (m/z) (MALDI-MS⁺) calculated for $C_{57}H_{45}N_6O_9EuK$ $m/z = 1147.2084$ [Eu(**1(R)**–H⁺)₃ + K⁺]⁺; found $m/z = 1147.2039$; ¹H NMR (600 MHz, CD₃CN, δ_H) ppm 9.19, 8.66, 8.32, 8.05, 7.86, 7.55, 7.25, 7.09, 6.30, 5.28, 4.67, 4.53, 4.30, 3.60, 3.08, 2.96, 2.72, 1.94, 1.70, 1.27, 0.88, 0.44, 0.04, −0.68, −1.27; IR ν_{max} (cm⁻¹): 3269, 3098, 1625, 1591, 1560, 1451, 1352, 1279, 1242, 1224, 1158, 1092, 1028, 905, 860, 820, 750, 732, 680, 661, 635, 575, 554, 542, 525; anal. calc. for 1.0 [$EuC_{60}H_{48}F_9N_6O_{18}S_3$]·1.3[$EuC_{57}H_{45}N_6O_9$] ([**Eu(1(R))₃(CF₃SO₃)₃**]· **1.3[Eu(1(R)–H)₃]**), %: C 53.8, H 3.2, N 6.4, S 3.4; found, %: C 53.6, H 3.6, N 6.4, S 3.2.

Acknowledgements

Notes and references

1 (a) M. C. Heffern, L. M. Matosziuk and T. J. Meade, *Chem. Rev.*, 2014, **114**(8), 4496–4539; (b) J.-C. G. Bünzli, *Chem. Rev.*, 2010, **110**, 2729–2755; (c) S. V. Eliseeva and J.-C. G. Bünzli, *New J. Chem.*, 2011, **35**, 1165–1176; (d) C. Lincheneau, F. Stomeo, S. Comby and T. Gunnlaugsson, *Aust. J. Chem.*, 2011, **64**(10), 1315–1326; (e) C. Lincheneau, B. Jean-Denis and T. Gunnlaugsson, *Chem. Commun.*, 2014, **50**, 2857–2860; (f) J.-F. Ayme, G. Gil-Ramírez, D. A. Leigh, J.-F. Lemonnier, A. Markevicius, C. A. Muryn and G. Zhang, *J. Am. Chem. Soc.*, 2014, **136**, 13142–13145.

2 (a) E. Pazos and M. E. Vázquez, *Biotechnol. J.*, 2014, **9**(4), 241–252; (b) N. Sim, S. Gottschalk, R. Pal, J. Engelmann, D. Parker and A. Mishra, *Chem. Sci.*, 2013, **4**, 3148–3153; (c) E. De Luca, P. Harvey, K. H. Chalmers, A. Mishra, P. K. Senanayake, J. I. Wilson, M. Botta, M. Fekete, A. M. Blamire and D. Parker, *J. Biol. Inorg. Chem.*, 2014, **19**, 215–227; (d) A. Mishra, R. Mishra, S. Gottschalk, R. Pal, N. Sim, J. Engelmann, M. Goldberg and D. Parker, *ACS Chem. Neurosci.*, 2014, **5**, 128–137; (e) N. H. Evans, R. Carr, M. Delbianco, R. Pal, D. S. Yufit and D. Parker, *Dalton Trans.*, 2013, **42**, 15610–15616; (f) S. J. Butler, M. Delbianco, N. H. Evans, A. T. Frawley, R. Pal, D. Parker, R. S. Puckrin and D. S. Yufit, *Dalton Trans.*, 2014, 5721–5730; (g) L. E. Buerkle and S. J. Rowan, *Chem. Soc. Rev.*, 2012, **41**, 6089–6102.

3 (a) G. Muller, *Dalton Trans.*, 2009, 9692–9707; (b) R. Carr, N. H. Evans and D. Parker, *Chem. Soc. Rev.*, 2012, **41**, 7673–7686; (c) S. Shinoda, *Chem. Soc. Rev.*, 2013, **42**, 1825–1835; (d) A. Indapurkar, B. Henriksen, J. Tolman and J. Fletcher, *J. Pharm. Sci.*, 2013, **102**(8), 2589–2598; (e) M. Ziegler and A. von Zelewsky, *Coord. Chem. Rev.*, 1998, **177**, 257–300; (f) U. Knof and A. von Zelewsky, *Angew. Chem., Int. Ed.*, 1999, **38**, 308–322.

4 (a) M. Cantuel, G. Bernardinelli, G. Muller, J. P. Riehl and C. Piguet, *Inorg. Chem.*, 2004, **43**, 1840–1849; (b) G. Bozoklu, C. Gateau, D. Imbert, J. Pécaut, K. Robeyns, Y. Filinchuk, F. Memon, G. Muller and M. Mazzanti, *J. Am. Chem. Soc.*, 2012, **134**, 8372–8375; (c) S. D. Bonsall, M. Houcheime, D. A. Straus and G. Muller, *Chem. Commun.*, 2007, 3676–3678; (d) K. N. T. Hua, J. Xu, E. E. Quiroz, S. López, A. J. Ingram, V. A. Johnson, A. R. Tisch, A. de Bettencourt-Dias, D. A. Straus and G. Muller, *Inorg. Chem.*, 2012, **51**, 647–660.

5 S. J. Bradberry, A. J. Savyasachi, M. Martínez-Calvo and T. Gunnlaugsson, *Coord. Chem. Rev.*, 2014, **273–274**, 226–241.

6 (a) A.-L. Gassner, C. Duhot, J.-C. G. Bünzli and A.-S. Chauvin, *Inorg. Chem.*, 2008, **47**, 7802–7812; (b) J. Andres and A.-S. Chauvin, *Inorg. Chem.*, 2011, **50**, 10082–10090.

7 J. P. Leonard, P. Jensen, T. McCabe, J. E. O'Brien, R. D. Peacock, P. E. Kruger and T. Gunnlaugsson, *J. Am. Chem. Soc.*, 2007, **129**, 10986–10987.

8 O. Kotova, J. A. Kitchen, C. Lincheneau, R. D. Peacock and T. Gunnlaugsson, *Chem.–Eur. J.*, 2013, **19**, 16181–16186.

9 (a) S. Comby, F. Stomeo, C. P. McCoy and T. Gunnlaugsson, *Helv. Chim. Acta*, 2009, **92**, 2461–2473; (b) F. Stomeo, C. Lincheneau, J. P. Leonard, J. E. O'Brien, R. D. Peacock, C. P. McCoy and T. Gunnlaugsson, *J. Am. Chem. Soc.*, 2009, **131**, 9636–9637; (c) C. Lincheneau, R. D. Peacock and T. Gunnlaugsson, *Chem.–Asian J.*, 2010, **5**, 500–504.

10 C. Lincheneau, J. P. Leonard, T. McCabe and T. Gunnlaugsson, *Chem. Commun.*, 2011, **47**, 7119–7121.

11 C. Lincheneau, C. Destribats, D. E. Barry, J. A. Kitchen, R. D. Peacock and T. Gunnlaugsson, *Dalton Trans.*, 2011, 12056–12059.

12 (*a*) J. A. Kitchen, D. E. Barry, L. Mercs, M. Albrecht, R. D. Peacock and T. Gunnlaugsson, *Angew. Chem., Int. Ed.*, 2012, **51**, 704–708; (*b*) D. E. Barry, J. A. Kitchen, M. Albrecht, S. Faulkner and T. Gunnlaugsson, *Langmuir*, 2013, **29**, 11506–11515.

13 (*a*) N. M. Shavaleev, F. Gumy, R. Scopelliti and J.-C. G. Bünzli, *Inorg. Chem.*, 2009, **48**, 5611–5613; (*b*) N. M. Shavaleev, R. Scopelliti, F. Gumy and J.-C. G. Bünzli, *Inorg. Chem.*, 2009, **48**, 6178–6191; (*c*) N. M. Shavaleev, S. V. Eliseeva, R. Scopelliti and J.-C. G. Bünzli, *Chem.–Eur. J.*, 2009, **15**, 10790–10802; (*d*) G. S. Kottas, M. Mehlstäubl, R. Fröhlich and L. De Cola, *Eur. J. Inorg. Chem.*, 2007, 3465–3468.

14 G. Pescitelli, L. Di Bari and N. Berova, *Chem. Soc. Rev.*, 2014, **43**, 5211–5233.

15 Y. Hamuro, S. J. Geib and A. D. Hamilton, *J. Am. Chem. Soc.*, 1997, **119**(44), 10587–10593.

16 P. K. Mandal and J. S. McMurray, *J. Org. Chem.*, 2007, **72**, 6599–6601.

17 A. Beeby, I. M. Clarkson, R. S. Dickins, S. Faulkner, D. Parker, L. Royle, A. S. de Sousa, J. A. G. Williams and M. Woods, *J. Chem. Soc., Perkin Trans. 2*, 1999, 493–503.

18 (*a*) C.-W. Cho and M. J. Krische, *Org. Lett.*, 2006, **8**(17), 3873–3876; (*b*) J. S. Bryans, D. C. Horwell, G. S. Ratcliffe, J.-M. Receveur and J. R. Rubin, *Bioorg. Med. Chem.*, 1999, **7**(5), 715–721; (*c*) Y.-T. Hong, C.-W. Cho, E. Skucas and M. J. Krische, *Org. Lett.*, 2007, **9**(19), 3745–3748; (*d*) J.-R. Kong, M.-Y. Ngai and M. J. Krische, *J. Am. Chem. Soc.*, 2006, **128**(3), 718–719.

19 A.-S. Chauvin, F. Gumy, D. Imbert and J.-C. G. Bünzli, *Spectrosc. Lett.*, 2004, **37**(5), 517–532; *Spectrosc. Lett.*, 2007, **40**, 193.

20 G. Canard, S. Koeller, G. Bernardinelli and C. Piguet, *J. Am. Chem. Soc.*, 2008, **130**, 1025–1040.

21 (*a*) H. Gampp, M. Maeder, C. J. Meyer and A. D. Zuberbühler, *Talanta*, 1986, **33**, 943–951; (*b*) H. Gampp, M. Maeder, C. J. Meyer and A. D. Zuberbühler, *Talanta*, 1985, **23**, 1133–1139.

22 T. Le Borgne, P. Altmann, N. André, J.-C. G. Bünzli, G. Bernardinelli, P.-Y. Morgantini, J. Weber and C. Piguet, *Dalton Trans.*, 2004, 723–733.

23 (*a*) N. Berova, L. Di Bari and G. Pescitelli, *Chem. Soc. Rev.*, 2007, **36**, 914–931; (*b*) G. A. Hembury, V. V. Borovkov and Y. Inoue, *Chem. Rev.*, 2008, **108**, 1–73.

24 (*a*) R. S. Dickins, J. A. K. Howard, J. M. Moloney, D. Parker, R. D. Peacock and G. Siligardi, *Chem. Commun.*, 1997, 1747–1748; (*b*) R. S. Dickens, J. A. K. Howard, C. L. Maupin, J. M. Moloney, D. Parker, R. D. Peacock, J. P. Riehl and G. Siligardi, *New J. Chem.*, 1998, 891–899; (*c*) G. Bobba, Y. Bretonnière, J.-C. Frias and D. Parker, *Org. Biomol. Chem.*, 2003, **1**, 1870–1872.

25 *Comprehensive chiroptical spectroscopy*, ed. N. Berova, P. L. Polavarapu, K. Nakanishi and R. W. Woody, Wiley-VCH, New York, 2012.

26 (*a*) S. G. Telfer, N. Tajima, R. Kuroda, M. Cantuel and C. Piguet, *Inorg. Chem.*, 2004, **43**, 5302–5310; (*b*) M. Albrecht, O. Osetska, T. Abel, G. Haberhauer and E. Ziegler, *Beilstein J. Org. Chem.*, 2009, **78**, 1–8; (*c*) S. Sairenji, S. Akine and T. Nabeshima, *Tetrahedron Lett.*, 2014, **55**, 1987–1990.

27 (*a*) *Bruker APEX v2012.12–0*, Bruker AXS Inc., Madison, Wisconsin, USA, 2012; (*b*) G. M. Sheldrick, *SHELXL-2013*, University of Göttingen, Germany, 2013.

28 G. F. de Sá, L. Nunez, Z. M. Wang and G. R. Choppin, *J. Alloys Compd.*, 1993, **196**, 17–23.

29 J. N. Demas and G. A. Crosby, *J. Phys. Chem.*, 1971, **75**, 991–1024.

30 M. H. V. Werts, R. T. F. Jukes and J. W. Verhoven, *Phys. Chem. Chem. Phys.*, 2002, **4**, 1542–1548.